RAPID COMMUNICATIONS

PHYSICAL REVIEW E VOLUME 50, NUMBER 3 SEPTEMBER 1994

# Pattern selection of multicrack propagation in quenched crystals

Yoshinori Hayakawa

*Research Institute of Electrical Communication, Tohoku University, Katahira, Aoba-ku, Sendai 980, Japan*

(Received 18 April 1994)

We study crack propagation in locally quenched crystals by two- and three-dimensional numerical simulations of a deterministic spring model. Controlling applied stress and material specific parameters, we find that a cellular structure bounded by cracks forms and the size of cells is selected through relaxation processes. We also find that numerical results are well represented with a scaling relation including two different regions of crack growth.

PACS number(s): 62.20.Mk, 81.40.Np, 75.70.Kw

When a brittle material at high temperature is quenched inhomogeneously, propagating cracks are often observed due to the thermal stress induced in the material. If the stress is applied with a localized temperature gradient and the distorted zone is continuously shifted in a direction at a constant velocity, resulting crack tips are expected to stay within or near the zone, as known for the growth fronts in directional solidification experiments [1]. Accordingly, the mean velocity and direction of propagating cracks can be controlled, unlike the ordinary crack formations by external loads. Recently Yuse and Sano [2] reported well-controlled experiments on the crack formation of glass plates by applying directional thermal stress. They prepared very thin glass plates and heated them up first. When the plate was dipped into cool water to make a directional load locally, they found a variety of propagating crack patterns including oscillatory and parallel straight cracks with good reproducibility. They also found that cracks choose an optimal spacing between them depending on control parameters [3] as seen in the wavelength selection of directional solidification. But the origin of the instability of crack growth and mechanism of the crack pattern selection still have not been understood well [4–8]. In this Rapid Communication we study a simple spring network model to describe the crack formation of a brittle material being inspired by those experiments. And we discuss the pattern selection caused by crack growth for two- and three-dimensional cases.

Let us consider first elastic properties of a simple cubic (or square) crystal, which is subject to thermal stress, with nearest-neighbor and next-nearest-neighbor interactions. Force applied between "atoms" in the crystal is assumed to be represented by Hookean springs, where the springs can be freely rotated around the atoms [9,10]. We do not take into account acoustic vibrations in the crystal at all, because the speed of cracks is thought to be extremely slower than that of sound in the phenomena we are concerned with here. Let $k_1$ be the spring constant for nearest-neighbor interactions and $k_2$ for next-nearest-neighbor interactions. Then one can easily obtain the components of elastic tensor $C_{ijkl}$ of the two-dimensional (2D) square crystal [11,12]:

$$C_{iiii}=k_1+k_2, \tag{1}$$

$$C_{iijj}=C_{ijji}=C_{ijij}=k_2, \tag{2}$$

and the other coefficients are zero. Here $i$ and $j$ exclusively take one of $x$ and $z$. For the three-dimensional simple cubic crystal with lattice constant $a_0$,

$$C_{iiii}=\frac{k_1+2k_2}{a_0}, \tag{3}$$

$$C_{iijj}=C_{ijji}=C_{ijij}=\frac{k_2}{a_0}, \tag{4}$$

where $i$ and $j$ are one of $x$, $y$, and $z$ as well. Note that the lattice constant $a_0$ of the spring network does not affect the elastic property in the two-dimensional system.

Thermal stress is applied to the crystal as in the experiments we mentioned. First we assume that temperature $T$ at each spring is given by the following function of "vertical" position $z$ and time $t$:

$$T(z,t)=-\frac{\Delta T}{2}\tanh\{\beta[z-z_0(t)]\}, \tag{5}$$

$$z_0(t)=Vt, \tag{6}$$

where $\Delta T$ is the temperature difference applied between the top and the bottom of the specimen, $V$ is the velocity of the zone where failure takes place. Here $\beta$ is a parameter that corresponds to the inverse of thermal diffusion length $d(=1/\beta) \simeq D/V$ ($D$ is the thermal diffusion constant). Since the system is assumed to be quasistatic, $\beta$ is the only parameter related to the dipping velocity $V$. In numerical simulations, we simplify (6) as $z_0(0)=\delta z n$, where $n$ is the number of iterative steps and $\delta z$ a small number compared to the lattice constant ($\delta z \simeq a_0/10$ in our simulations). According to the temperature distribution, the equilibrium length $a_0(z)$ of springs is determined as

$$a_0(z,n)=a_0[1+\alpha T(z,n)], \tag{7}$$

where $a_0$ is the lattice constant of stress-free crystal and $\alpha$ the thermal expansion coefficient. Since the springs have an extent, temperature is evaluated at the middle point of each spring.

If the spring network is not in its equilibrium configuration, the restitutive force $\mathbf{F}$ at node $i$ is represented by

1063-651X/94/50(3)/1748(4)/$06.00

$$\mathbf{F}_i = \sum_{j \in \text{n.n.}} k_1 \frac{\mathbf{r}_i - \mathbf{r}_j}{|\mathbf{r}_i - \mathbf{r}_j|}[a_0(z,n) - |\mathbf{r}_i - \mathbf{r}_j|] + \sum_{j \in \text{n.n.n.}} k_2 \frac{\mathbf{r}_i - \mathbf{r}_j}{|\mathbf{r}_i - \mathbf{r}_j|}[a_0(z,n) - |\mathbf{r}_i - \mathbf{r}_j|], \quad (8)$$

where n.n. denotes nearest-neighbor nodes and n.n.n. next-nearest-neighbor nodes. The equilibrium configuration of the springs network is then calculated by a simple relaxation method so that $\mathbf{F}_i = \mathbf{0}$ at every node $i$. In our simulations, relative error of the displacement of nodes was smaller than $10^{-4}$.

Here we introduce a deterministic rule for breaking springs (bonds) [13,14], rather than stochastic ones [15–17], according to the applied thermal stress. When the force given on a spring exceeds a critical value, it breaks, i.e., the corresponding spring constant changes from $k_1$ or $k_2$ to zero, which can be regarded as a microscopic interpretation of the failure criterion for an ideal brittle material [18]. Let $f_c$ be the critical force for breaking the bonds. In short, the following procedure is carried out in each time step $n$: "Calculate the force for every bond. If more than one bond have loads larger than $f_c$, break one which has the maximum force and do the relaxation processes to find an equilibrium configuration again, until no bond is broken."

Computer simulations were carried out for both 2D and 3D cases. In our 2D simulations rectangles of up to $256 \times 512$ nodes are used as model specimens to be broken. For 3D cases, we carried out simulations with rectangular parallelpipeds of up to $48 \times 48 \times 48$ nodes. On the boundaries of the specimens, no constraint is applied to the motion of nodes. In the continuum limit of this model, therefore, external pressure on the boundaries is zero. As the parameters related to elastic property, we choose $k_1 = 1$, $k_2 = 0.7$ for 2D, and $k_1 = 1$, $k_2 = 0.5$ for 3D, in the following study. From the consideration of direction dependency of Young's modulus $E$, one can find that the elasticity of the model materials is anisotropic with these values. As long as we used a modest ratio of $k_1/k_2$, say 0.5–2, we could not find apparent differences in resultant patterns. However, in general, we expect that the preferred direction of crack propagation can be controlled by changing this ratio [8]. Furthermore, the growth direction may also be influenced by lattice anisotropy during failure, as known in diffusion-limited aggregation (DLA) on a lattice [10]. The effects of such anisotropic properties of materials on the crack formation, especially in a large size system, is one of the issues for our future study.

A number of tiny cracks were prepared randomly at the bottom of the lattice to make initiation of cracks easier. For small applied thermal stress, the initial cracks do not grow at all. Increasing it, a transition from nonpropagating cracks to propagating cracks takes place, and cracks run in the $z$ direction dividing the lattice into several pieces. According to control parameters such as $\alpha$ and $d(=1/\beta)$, the cracks seem to autonomously choose their mutual positions or the number of domains bounded by them (see Figs. 1 and 2). In Fig. 1, two typical crack patterns are shown for different thermal diffusivities. Here let $\lambda$ be the typical (mean) domain size separated by the cracks. Since propagating cracks are repulsive to each other in our model, they do not merge in 2D cases, while crack planes in 3D may intersect when the angle between them is sufficiently large. Therefore, with too many initial cracks, there are competitions between them, e.g., a screening effect of cracks as seen in DLA, and some of the branches will survive at the end. On the other hand, if the number of initial cracks is fewer than an optimal number, nucleation of crack tips (planes) occurs and some of the running cracks split to adjust the number. Even without initial cracks, initiation of cracks occurs near the center of the strip, and then the crack grows and splits. That is, there is a selection mechanism of $\lambda$, and the cracks can choose it by themselves from any initial conditions.

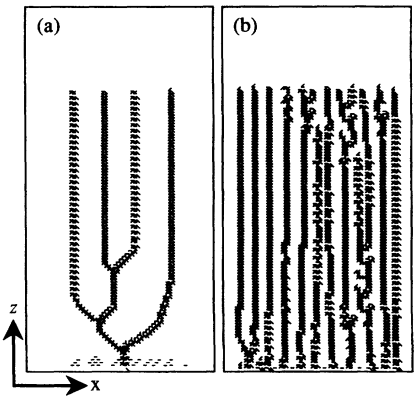


FIG. 1. Typical two-dimensional crack patterns for $a_0 = 1$, $d = 1$, $\Delta T = 2$, $f_c = 0.0025$, and (a) $\alpha = 0.005$ (b) $\alpha = 0.02$. Only broken bonds are shown.

Propagating cracks may have some degree of freedom in their configurations by changing the vertical ($z$) position of the tips and morphology of the individual cracks other than horizontal spacing $\lambda$. In fact, in the steady state of crack growth in 2D, spontaneous branching and oscillatory motion of cracks are observed, probably because of the frustration between different stable configurations. And such behavior of crack tips has a nonlocal effect which seems to initiate instabilities of the neighbor cracks as seen in Fig. 1(b). In those cases, for a given set of parameters, the obtained values of $\lambda$ have some deviation along with a mean value over time.

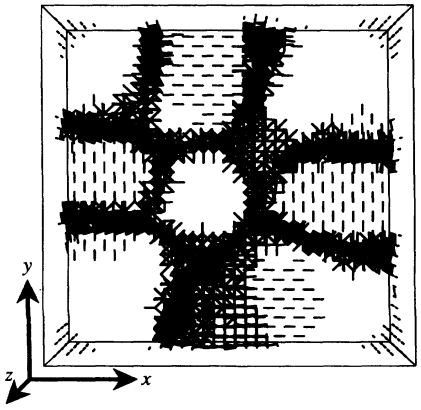


FIG. 2. Three-dimensional view of a typical three-dimensional crack pattern. Broken bonds are shown for $a_0 = 1$, $\alpha = 0.0085$, $\Delta T = 2$, $d = 1$, and $f_c = 0.0025$.

For straight cracks as shown in Fig. 1(a), $\lambda$ can be determined uniquely in its steady state, though the selected $\lambda$ seems to be slightly influenced by initial conditions, i.e., the number of initial cracks, as shown by numerical evidence. However, the deviation arising from initial conditions gives a minor contribution to spacing selection in our numerical simulations. With this discrete modeling of extremely brittle material, nucleation of new crack tips can take place easily even without additive noise. If the initiation of new cracks needs large activation energy, that is likely in real homogeneous materials, crack configuration may be trapped in a metastable state, and the resultant $\lambda$ would be more sensitive to initial conditions. We would like to discuss later how $\lambda$ is determined in our simulations.

In 3D, the time required to enter the steady state seems to be much shorter than that in 2D, and the deviations of $\lambda$ seem to be also smaller. In this case, the cracks take a columnar structure grown in the $z$ direction as shown in Fig. 2, whose diameter depends on control parameters. We define $\lambda$ as the average diameter which is evaluated from the average area per each cell by taking cross sections of the 3D lattice in the $x$-$y$ plane. Unfortunately we could not present here the distribution profile of $\lambda$, which seems to have a sharp peak, owing to our very limited system size.

In order to characterize size selection during crack formation, we define a couple of independent dimensionless parameters in this model. One is the ratio of thermal diffusion length and $\lambda$ defined as

$$L=\beta\lambda=\frac{\lambda}{d}, \tag{9}$$

and the other is

$$R=\frac{\alpha\Delta T E a_0^{n-3/2}\lambda^{1/2}}{f_c}, \tag{10}$$

where $E$ is Young's modulus which may depend on the direction of the applied force, $n$ the dimension of space. Critical force $f_c$ is related to the critical stress intensity factor $K_I^c$ of the material as $K_I^c \simeq f_c/a_0^{n-3/2}$, thus $R$ should be identical, except for some numerical factor, to that introduced by Sasa *et al.* in their theoretical stability analysis of propagating cracks [7]. That is, using $K_I^c$, the second dimensionless parameter could be written as $R'=\alpha\Delta T E\sqrt{\lambda}/K_I^c$ in terms of conventional fracture mechanics. Physical interpretation of the parameter $R$ is, therefore, the ratio of the critical stress intensity factor (tolerance of material) and the external load in the same form as $K_I$.

Let us assume the following relation between $R$ and $L$:

$$1/R=f(L), \tag{11}$$

where $f(L)$ is a function which saturates for large $L$, because $1/R$ should not diverge for a finite applied load even when $L\to\infty$. Using $L$ and $R$, the crack pattern in Fig. 1(a) was obtained for $L=12.8$, $R=0.050$, Fig. 1(b) for $L=4.9$, $R=0.020$, and Fig. 2 for $L=6.9$, $R=0.010$. In Fig. 3, the relation between $L$ and $1/R$ is shown for several independent numerical results by changing $\alpha$ and $d(=1/\beta)$ as control parameters. In the plot, we also present the data for which

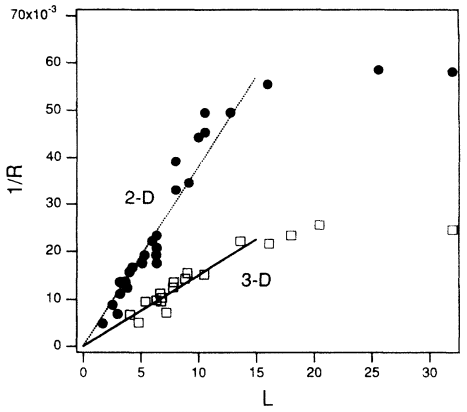


FIG. 3. Scaling plot of numerical results by changing $\alpha$ and $d(=1/\beta)$ as control parameters. $\alpha$ is in the range between 0.003 and 0.02, $\beta$ between 0.02 and 1.5. Each point corresponds to independent computer simulations. Black circles represent the results for 2D and white rectangles for 3D.

only initial numbers of cracks were different. As seen in the figure, all independent data fall into a curve and Eq. (11) represents the numerical results well in both 2D and 3D cases. Although the scatter of the points seems to be large due to deviations of resultant $\lambda$, looking at Fig. 3, there is a linear region in $f(L)$ for $L<10$, and it gradually saturates to a constant value for large $L$. In other words, there are at least two characteristic regions of crack growth, say, thermal-diffusion-limited ($L<10$) and temperature-difference-limited ($L>10$) regions. Thus the asymptotic form of the scaling function $f$ would be

$$f(L)=\begin{cases} L^{\gamma} & \text{for small } L, \\ \text{const} & \text{for large } L, \end{cases} \tag{12}$$

where $\gamma\approx 1$ in our model. The dependency of $\gamma$ on models, however, has to be studied as well as the comparison with experiments. In glass experiments [2,3], $L$ is usually larger than 10 because it is not easy to have glass plates cooled down uniformly in the air with a long thermal diffusion length. Thus the crossover mentioned above may be hardly observable in real cases. Unfortunately to our knowledge the quantitative relationship between $R$ and $L$ for multicrack ex-

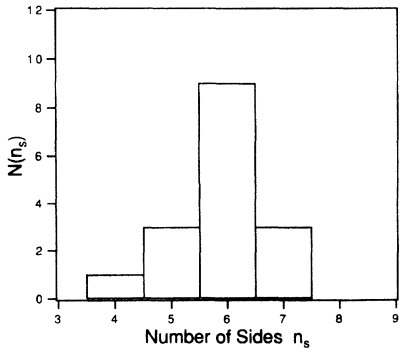


FIG. 4. Distribution of the number of sides. Eighteen cells obtained from six independent simulations are examined to make this plot.

periments has not been reported so far. If $\lambda=1$, $\lambda\sim d^{2/3}$, making other parameters fixed for $L<10$. For very small $d$, i.e., with less thermal diffusivity, $\lambda$ will not depend on $d$. When $\Delta T$ is chosen as a control parameter, our results yield that $\lambda\sim\Delta T^{-2/3}$ for small $L$, otherwise $\lambda\sim\Delta T^{-2}$.

Directional crack propagation in 3D has an aspect of grain growth in 2D [19], because the 2D section of the three-dimensional column has a cellular structure which resembles grain structures frequently seen in nature and the structure forms in a relaxation process. From this point of view, columnar joints of rocks are thought to be one example of grain growth induced by crack propagation in 3D. Distribution of cell shape is one of the important measures to characterize cellular structure in grain growth problems. We took the intersection of the three-dimensional column in the $x$-$y$ plane, and counted the number of sides of cells $n_s$ for several independent computer runs. In Fig. 4, the histogram of $n_s$ is shown, where the cells facing boundaries were excluded from the counting. It is clear that a hexacylindrical shape is selected during the formation of the cellular structure even when the material is anisotropic. This indicates the existence of an effective surface tension to make the crack surface smaller. Dynamics of the grain growth caused by cracks, which might be an interesting topic, is our future problem.

To summarize this Rapid Communication, we have performed computer simulations of two- and three-dimensional crack propagation using a deterministic spring network model. We found that the spring network model works successfully for the fracture formation of brittle materials. In directional crack propagation, a cellular structure forms in the steady state, and the characteristic size of cells is well represented by a scaling relation that has a crossover at (crack separation)/(diffusion length) $\simeq 10$. We also discussed 3D directional crack formation as a problem of grain growth.

We would like to acknowledge M. Sano, S. Sasa, K. Sekimoto, and Y. Sawada for helpful discussions and suggestions. Y. Couder and H. J. Herrmann helped us with comments and encouragement to this study.

[1] *Dynamics of Curved Fronts*, edited by P. Pelcé (Academic, Boston, 1988).
[2] A. Yuse and M. Sano, Nature (London) **362**, 329 (1993).
[3] M. Sano, A. Yuse, Y. Sawada, and Y. Couder (unpublished).
[4] M. Marder (unpublished).
[5] Y. Taguchi (unpublished).
[6] H. Furukawa, Prog. Theor. Phys. **90**, 949 (1993).
[7] S. Sasa, K. Sekimoto, and H. Nakanishi, Phys. Rev. E **50**, R1733 (1994).
[8] Y. Hayakawa, Phys. Rev. E **49**, 1804 (1994).
[9] *Statistical Models for the Fracture in Disordered Media*, edited by H. J. Herrmann and S. Roux (North-Holland, Amsterdam, 1990).
[10] T. Vicsek, *Fractal Growth Phenomena*, 2nd ed. (World Scientific, Singapore, 1991).
[11] R. P. Feynman, R. B. Leighton, and M. Sands, *Lectures on Physics* (Addison-Wesley, Reading, MA, 1964), Vol. 2.
[12] L. D. Landau and E. M. Lifshitz, *Theory of Elasticity* (Pergamon, New York, 1959).
[13] L. Fernandez, F. Guinea, and E. Louis, J. Phys. A **21**, L301 (1988).
[14] H. J. Herrmann, J. Kertész, and L. de Arcangelis, Europhys. Lett. **10**, 147 (1989).
[15] S. Feng and P. N. Sen, Phys. Rev. Lett. **52**, 216 (1984).
[16] E. Louis and F. Guinea, Europhys. Lett. **3**, 871 (1987).
[17] P. Meakin, G. Li, L. M. Sander, E. Louis, and F. Guinea, J. Phys. A **22**, 1393 (1989).
[18] B. Lawn, *Fracture of Brittle Solids*, 2nd ed. (Cambridge University Press, Cambridge, England, 1993).
[19] H. V. Atkinson, Acta Metall. **36**, 469 (1988).

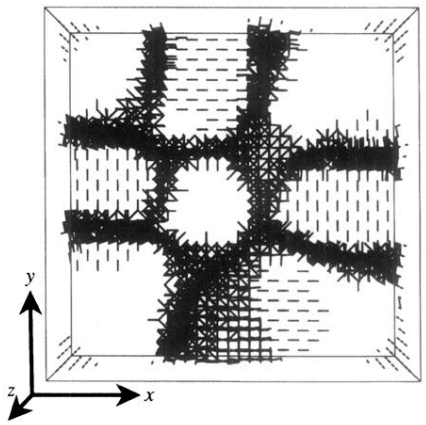


FIG. 2. Three-dimensional view of a typical three-dimensional crack pattern. Broken bonds are shown for $a_0=1$, $\alpha=0.0085$, $\Delta T=2$, $d=1$, and $f_c=0.0025$.